Solid State Ionics 3/4 (1981) 365–371
North-Holland Publishing Company

INTERFACIAL PHENOMENA OF SOME FLUORITES

J. SCHOONMAN, L.J. STIL
Solid State Department, Physics Laboratory, State University of Utrecht, 3508 TA Utrecht, The Netherlands

J.R. MACDONALD
Department of Physics and Astronomy, University of North Carolina, Chapel Hill, NC 27514, USA

and

D.R. FRANCESCHETTI
Physics Department, Memphis State University, Memphis, TN 38152, USA

The small-signal ac response of symmetrical cells with β-PbF_2 and $Pb_{1-x}Bi_xF_{2+x}$ ($x \leq 0.05$) as solid electrolyte and Pt or Au electrodes has been studied in the frequency range 10^{-4} Hz to 50 kHz between 25 and 450°C in ambients containing oxygen. Usually a complex-frequency-dependent interface impedance of the form $Z = K(i\omega)^{-\alpha}$ has been used to model the ac response for frequencies higher than 10^{-2} Hz. This study shows that the system response can be accurately modeled by a theoretical circuit, which takes finite-length Warburg effects, adsorption and electrode reaction effects into account in an explicit manner. For moderate temperatures $K(i\omega)^{-\alpha}$ leads to better fits than the finite-length Warburg element. The effect of oxygen is emphasized. Theoretical work based on electrode reactions involving oxygen has led to variations of the basic ladder network while retaining the finite-length Warburg element. Preliminary fit results indicate the possibility to distinguish between diffusion processes in the electrode and in the electrolyte.

1. Introduction

Cubic lead fluoride, β-PbF_2, and solid solutions based on β-PbF_2 are among the best anion-conducting solid electrolytes known to date [1,2]. Their ionic and electronic conductivity parameters have been characterized in great detail [3–5].

Electrode processes of β-PbF_2 have been studied by cyclic voltammetry [6], and small-signal ac response measurements [7,8]. Raistrick et al. [7] have found the frequency-dependent impedance

$$Z = A\omega^{-\alpha} - iB\omega^{-\alpha} \qquad (1)$$

to describe the small-signal ac response of the interface between polished β-PbF_2 crystals and sputtered Pt or Au electrodes in inert ambients. The Kramers–Kronig relation leads to the relation $B = A\tan(\alpha\pi/2)$ for the coefficients in eq. (1) [7,9]. With this relation one finds that eq. (1) becomes the constant-phase-angle (CPA) impedance,

$$Z = K(i\omega)^{-\alpha}, \qquad (2)$$

so that $A = K\cos(\pi\alpha/2)$, and $B = K\sin(\pi\alpha/2)$. The numerical data for Au electrodes [7] lead to the relation $\log A = (1.46 \pm 0.21)\log B - (4.19 \pm 1.46)$, which is not consistent with this important constraint. The non-Debye bulk and interface capacitances as observed for pressed pellets of β-PbF_2 in contact with Au [8] are concordant with the constant-phase-angle impedance.

Raistrick et al. [7] ascribe the frequency-dependent impedance given by eq. (1) to energy storage and dissipation effects ($D = A/B$) at the interface. Jonscher and Réau [8] apply to their data for polycrystalline β-PbF_2 Jonscher's screened hopping conduction model, i.e. mutual

0167–2738/81/0000–0000/$02.50

interactions between hopping charge carriers which lead to a frequency-dependent mobility. However, at 200°C, the maximal temperature in the Jonscher–Réau study, the fluoride ion vacancy concentration [3, 4] is a factor of 10^2 smaller than the concentration for which defect interactions are to be expected [10].

This paper presents a study of the small-signal ac response of single crystals of β-PbF_2, and anion-excess solid solutions $Pb_{1-x}Bi_xF_{2+x}$ with Pt and Au as inert electrodes, and in ambients which contain oxygen. It is shown that a unified treatment of diffusion processes at the electrode/electrolyte interface [11], which is afforded by the formalism of complex frequency-dependent rate constants [12–14] often allows an adequate interpretation of the system response.

2. Experimental aspects

2.1. Materials

The growth of single crystals of undoped β-PbF_2 has been reported [3]. Single crystals of $Pb_{1-x}Bi_xF_{2-x}$ ($x \leq 0.05$) were grown from mixtures of α-PbF_2 (Merck, ultra pure), and BiF_3 (Baker, analytical grade) in a graphite container placed in a quartz tube in a conventional zone-refining apparatus. A mixed ambient of HF and dried oxygen-free N_2 was maintained in the quartz tube during zone-leveling, and crystal growth. The HF ambient was generated in the quartz tube by heating a teflon filled graphite boat placed next to the fluoride mixture. Single crystalline ingots, 6×10^{-2} m long, and 8×10^{-3} m in diameter, were obtained. Small disks were cut from the ingots, and polished to optical finish. The polished surfaces were covered with Pt-paint electrodes (Leitplatin, Degussa). In addition sputtered Pt and Au electrodes were employed (Edwards S150 sputter coater).

2.2. Small-signal ac measurements

The symmetric cells were springloaded between platinum disks in an evacuable stainless-steel conductivity cell, equipped with resistance heating and a temperature controller. Oxygen partial pressures ranged from 4.98×10^{-4} Pa, in the inert ambient used in this study, to 1.245×10^3 Pa.

The frequency dispersion of the ac electrical response of the cells was studied from 25 to 450°C over the frequency range 10^{-4} Hz–50 kHz, using a Wayne–Kerr autobalance bridge B641 in combination with a Rhode and Schwartz oscillator/detector SUB (50 Hz–50 kHz), and a frequency response analyser (Solartron 1172, input impedance 1 MΩ) (10^{-4} Hz–10 kHz). The ac signal amplitude was kept below 20 mV rms. *RC* simulation networks were measured in the frequency range involved, in order to check the reliability of the bridges, and the data fitting procedures [15].

3. Analysis of admittance data

In the present study the reaction of oxygen with the fluorites is taken into account. Oxygen may participate in the interfacial charge transfer by a number of mechanisms. The reaction

$$V_F^{\cdot} + O_{ads} + 2e' \rightleftharpoons O_F' \tag{3}$$

is likely for pure PbF_2, but the reaction

$$V_i^{\times} + O_{ads} + 2e' \rightleftharpoons O_i'' \tag{4}$$

and/or

$$F_F^{\times} + O_{ads} + e' \rightleftharpoons O_F' + \tfrac{1}{2}F_2 \tag{5}$$

are more probable for the extrinsic region in $Pb_{1-x}Bi_xF_{2+x}$, in which the free mobile fluoride ion vacancy concentration is negligibly small. In pure PbF_2 transport of oxygen may occur via a vacancy mechanism or through the diffusion of an $(O_FV_F)^{\times}$ pair, while at high temperatures [3, 4] an intersticialcy process $O_F' + F_i' \rightleftharpoons O_i'' + F_F^{\times}$ may occur. The latter process seems reasonable for the anion-excess solid solutions at all temperatures. A complete treatment of the system ac response must take into account the kinetics of oxygen transport both in the electrolyte and through the electrode as well as the kinetics of the electrode reaction itself.

Recently, the exact treatment of the small-signal ac response of unsupported systems has been generalized to allow for the rate-limiting diffusion of the product species of an electrode adsorption/reaction sequence into the electrolyte or through a planar electrode [11]. For the case of a single mobile charge carrier species the equivalent circuit of fig. 1a should suffice. The following relations hold for the circuit elements which represent the electrode reaction and adsorption processes [11]:

$$R_R = 2kT/z_p^2 e^2 p_0 k_{1f}, \tag{6}$$

$$C_A = (R_R k_{1b})^{-1}, \tag{7}$$

$$R_A = R_R k_{1b}/k_{3f}, \tag{8}$$

$$Z_D = Z_{DO}(i\omega H^2)^{-1/2} \tanh(i\omega H^2)^{1/2}, \tag{9}$$

where the k denote effective rate constants,

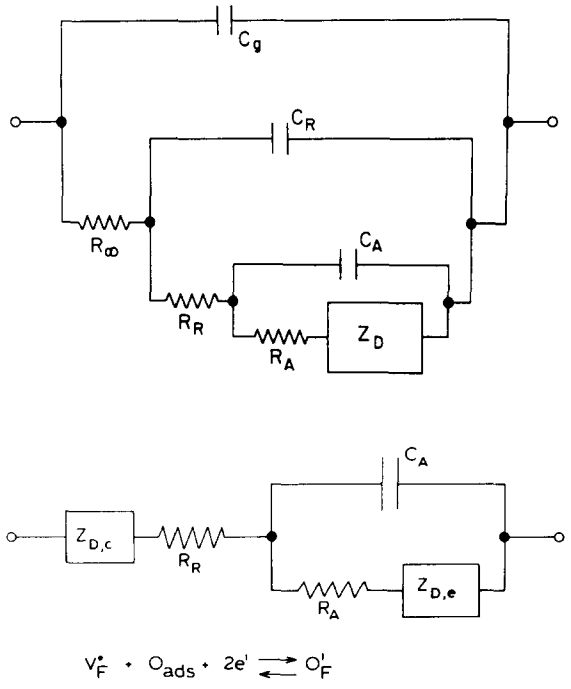

Fig. 1. (a) Equivalent circuit used for data analysis. C_g = geometric capacitance, R_∞ = bulk resistance, C_R = (diffuse double layer capacitance $-C_g$), R_R = electrode reaction resistance, R_A, C_A = adsorption process, Z_D = diffusional impedance. See text. (b) Theoretical equivalent circuit derived on the basis of reaction (3). $Z_{D,e}$ ≡ diffusion in electrode, $Z_{D,c}$ ≡ diffusion in crystal.

$H = \delta/D^{1/2}$, and

$$Z_{DO} = R_R k_{1b} k_{3b} \delta / k_{3f} D, \tag{10}$$

with δ a diffusion length, and D a diffusion constant. A circuit of this form is also appropriate when finite-length Warburg effects arise from processes in the electrolyte [14, 16].

Both the circuit of fig. 1a, and a modified circuit in which Z_D is taken to have the constant-phase-angle form $K(i\omega)^{-\alpha}$ have been incorporated into existing computer programs for the non-linear weighted least-squares analysis of complex data [17]. In the present study the data were weighted with their experimentally determined standard errors. Both the computer program of Macdonald and Garber, and a minimization method reported by Fletcher and Powell [18] were used to fit simultaneously the real and imaginary parts of the measured impedance or admittance to the equivalent circuit.

It should be noted that, in principle, the equivalent circuit of fig. 1a represents an oversimplification of the electrical response to be expected from the electrode reactions (3)–(5), in that it does not allow for the simultaneous diffusion of oxygen in the electrolyte and the electrode. One of the authors has recently derived a more general circuit, shown in fig. 1b for a system with electrode reaction (3), which will be discussed briefly below and more thoroughly in forthcoming work [19].

4. Experimental results and discussion

In fig. 2 complex-impedance data are shown for pure β-PbF_2 with Pt-paint electrodes in an ambient containing oxygen. For both painted and sputtered electrodes the impedance plots appear to curve to intersect the real axis as the frequency goes to zero. This was observed irrespective of whether β-PbF_2 or $Pb_{1-x}Bi_xF_{2+x}$ ($x \leq 0.05$) was used as solid electrolyte in ambients containing partial oxygen pressures ranging from $\approx 5 \times 10^{-4}$ Pa to $\approx 1.3 \times 10^3$ Pa.

At low and moderate temperatures system impedances were too high to allow measurements at the extreme low frequencies. Fig. 3

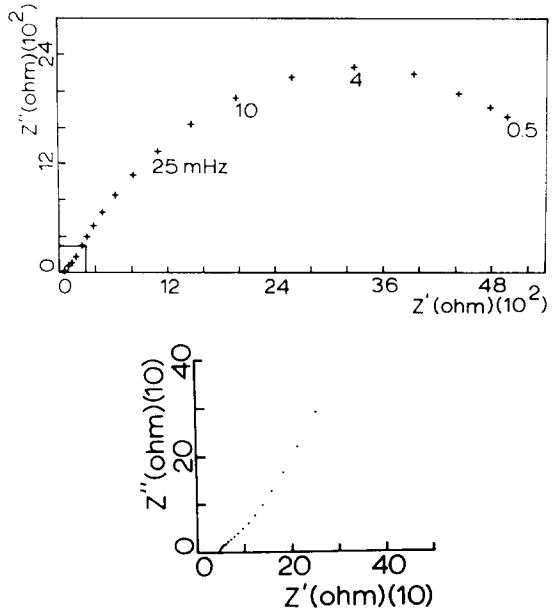

Fig. 2. Impedance plot for the cell Pt|β-PbF_2|Pt at 417°C. Oxygen partial pressure 10 Pa. Frequency range 5×10^{-4} Hz–10 kHz. Cell constant (l/O) 62.4 m^{-1}. Detailed high-frequency portion is shown separately.

presents complex-impedance data for $Pb_{0.987}Bi_{0.013}F_{2.013}$ with sputtered Pt electrodes at 19°C, while in fig. 4 complex-admittance data are presented for this solid electrolyte with sputtered Au electrodes at 212.3°C. Data for pure β-PbF_2 with Pt-paint electrodes have been fitted to the ladder network given in fig. 1a with for Z_D the finite-length Warburg element. Although the data in figs. 3 and 4 can be fitted to this ladder network with reasonable success, much better fits were obtained when for Z_D the CPA-impedance was employed. Results of the fit-procedures have been included in figs. 3 and 4. From the temperature dependence of fitted parameters activation enthalpies were obtained. For the finite-length Warburg impedance the temperature dependence of the effective Warburg constant Z_{EW} ($= Z_{DO}/H$) was considered. The enthalpies are gathered in table 1. The enthalpy values for R_∞ are equal to reported values [3, 4].

The temperature dependences of the circuit parameters can be used to test the reasonable-

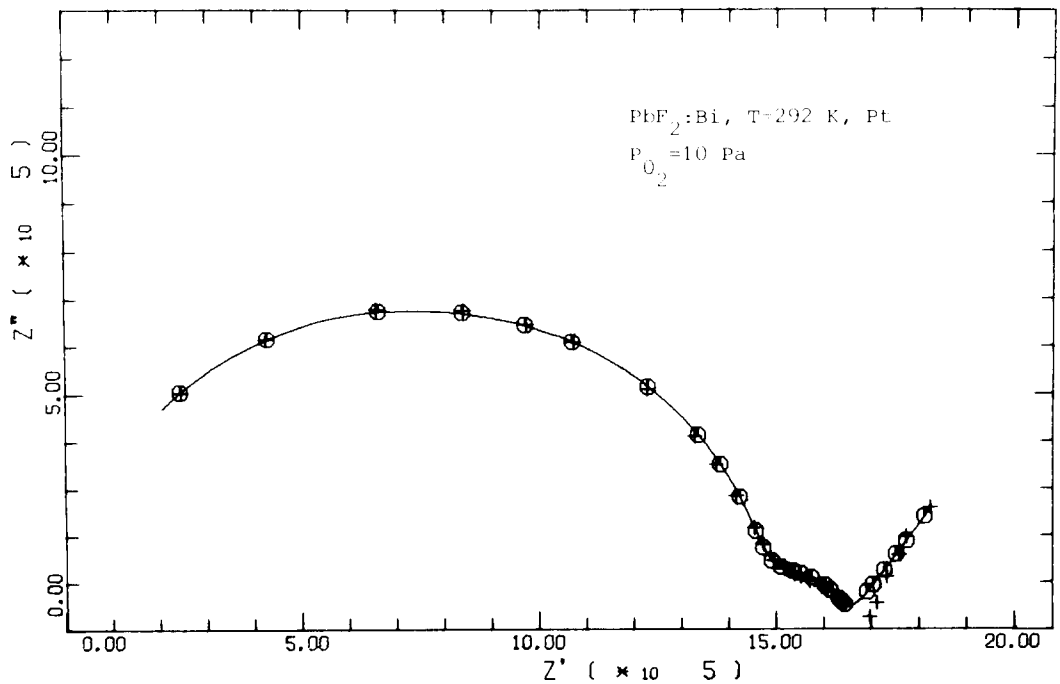

Fig. 3. Impedance plot for the cell Pt|$Pb_{0.987}Bi_{0.013}F_{2.013}$|Pt at 19°C. P_{O_2} = 10 Pa. Frequency range 1 Hz–45 kHz. Cell constant 64.096 m^{-1}. + experimental data; ○ equivalent-circuit fitting.

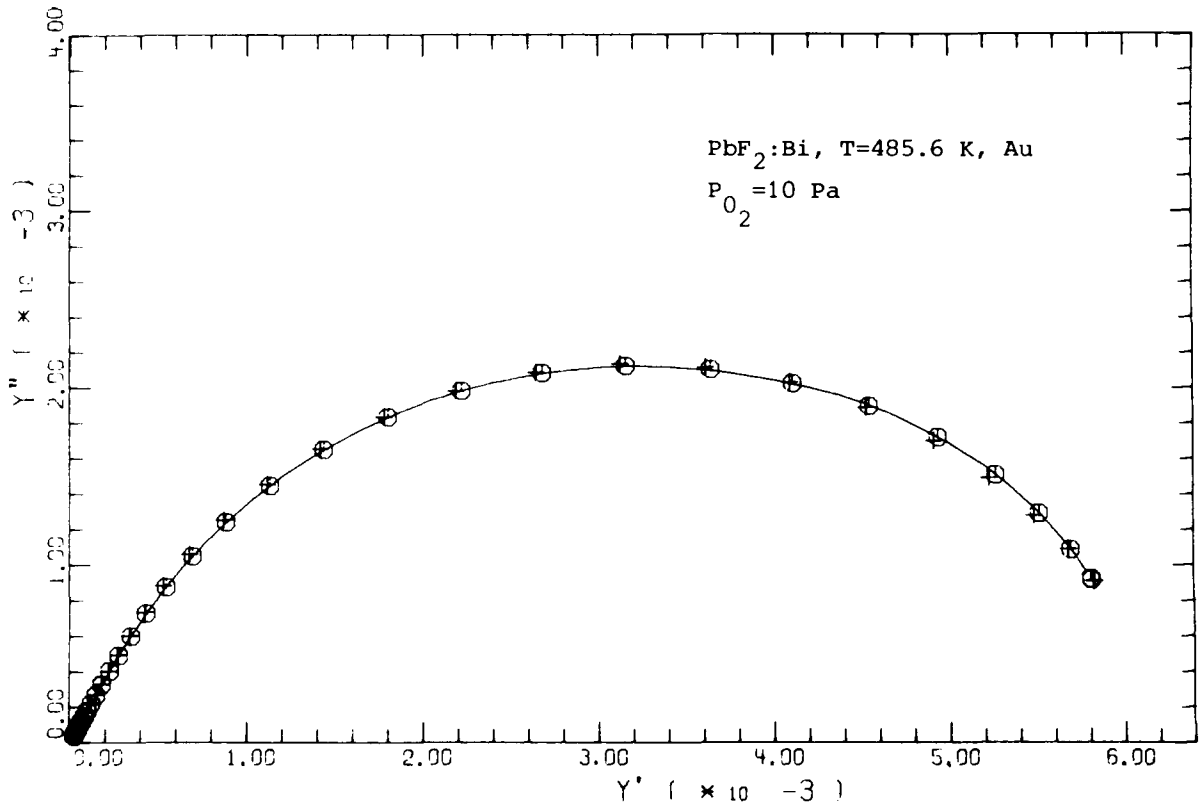

Fig. 4. Admittance plot for the cell Au|$Pb_{0.987}Bi_{0.013}F_{2.013}$|Au at 212.3°C. P_{O_2} = 10 Pa. Frequency range 1 Hz–10 kHz. Cell constant 56.237 m^{-1}. + experimental data; O equivalent-circuit fitting.

ness of the theoretical model underlying eqs. (6)–(9). From these equations we have that $\log R_R = \log R_A - \log(k_{1b}/k_{3f})$ and $\log C_A = -\log R_R - \log k_{1b}$. If the activation enthalpies associated with the effective rate constants k_{1b} and k_{3f} are sufficiently small, plots of $\log R_R$ against $\log R_A$ and of $\log C_A$ against $\log R_R$ should yield straight lines. Our data yield $\ln R_R = \ln R_A - 1.02$ for Au electrodes and $\ln R_R = \ln R_A - 1.57$ for Pt electrodes, and $\ln C_A = -0.66 \log R_R - 1.01$ for Au electrodes and $\ln C_A = -\ln R_R - 6.90$ for Pt electrodes. Only the C_A–R_A relation for Au electrodes contradicts the theoretical model, and the coefficient $0.66 \approx 2/3$ appearing in the observed relation strongly suggests that the origin of the discrepancy lies in a higher-order rate law for the electrode reaction than is assumed in the model. This point will be investigated in future theoretical work.

Table 1
Activation enthalpies (in eV) for the circuit elements as obtained from the non-linear complex least-squares analysis

Element	Undoped β-PbF_2	$Pb_{0.987}Bi_{0.013}F_{2.013}$	
	Pt-paint	sputtered Pt	sputtered Au
R_∞	0.67	0.556	0.542
C_R	–	0.257	0.262
R_R	0.85	0.425	0.493
C_A	0.95	0.265	0.216
R_A	0.78	0.315	0.378
K	–	0.223	0.296
Z_{EW}	0.88	–	–

The numerical values for C_A and C_R reveal differences for the different electrode materials. For Pt-paint electrodes C_A is larger than C_R by

a factor of ≈10, while for the sputtered Au and Pt electrodes C_A and C_R are about equal. This may be related to the more open structure of paint electrodes. The value of the constant-phase-angle exponent α varies between 0.55 and 0.82 for the different electrodes. These values are not reproducible on thermal cycling, except above ≈160°C for Au and 280°C for Pt. A sharp discontinuity in α occurs at ≈330°C, at which point rapid oxygen incorporation into the lattice is observed, as is manifested by a lowering of the bulk ionic conductivity of $Pb_{1-x}Bi_xF_{2+x}$, and a coloration of even the bulk of the crystals.

The activation enthalpies in table 1 reveal for K values which are smaller than 0.35 eV as found for A and B in eq. (1) [7]. However, a direct comparison is not possible, viz. eqs. (1) and (2). For the pure crystal Z_{EW} reveals an enthalpy value of 0.88 eV. The temperature dependence of Z_{EW} is governed by the concentration p_O [eq. (6)] and the diffusion coefficient D [eq. (10)] of the diffusing species, i.e. $Z_{EW}:(p_O D^{1/2})^{-1}$. This enthalpy value cannot be related to any of the mobile ionic or electronic species in β-PbF_2. If we assume reaction (3) to take place and $[V_F^{\cdot}]$ to be governed by the intrinsic anti-Frenkel defect formation constant [3,4] we obtain for the diffusion enthalpy of presumably oxygen the value 0.80 eV.

As a detailed physical model for the constant-phase-angle impedance is still lacking, the enthalpy values for K cannot be interpreted. The present study indicates, however, that the impedance must be related to oxygen diffusion. It should be noted, that the high-temperature conductivity of the solid solutions indicates the consumption of mobile F interstitials by reaction with oxygen. Besides the electrodes reactions (3)–(5), the direct reactions

$$\tfrac{1}{2}O_2 + 2F_i' \rightarrow O_i'' + F_2 + V_i^{\times} \qquad (11)$$

and

$$\tfrac{1}{2}O_2 + F_F^{\times} + F_i' \rightarrow O_F' + V_i^{\times} + F_2 \qquad (12)$$

must be considered.

At ≈200°C and $P_{O_2} = 10$ Pa the value of H is ≈1.28 for both β-PbF_2 with Pt-paint electrodes and the solid solution with sputtered Au electrodes. Taking into account the thickness of the electrode ($\delta \approx 100$ nm) or the crystal ($\delta \approx 2 \times 10^{-3}$ m) we obtain for the diffusion coefficient of oxygen through the electrode $\approx 6 \times 10^{-15}$ m²/s and in the crystal $\approx 2.5 \times 10^{-6}$ m²/s. While the former value is quite reasonable and possibly somewhat small, the latter is unreasonably large, and points to the need for the more complete treatment mentioned earlier, in which both transport processes are simultaneously taken into account. The experimental conditions lead to oxide ions in the interfacial region, even at the lowest applied oxygen partial pressures. To consider more completely the possibility of rate-limiting oxygen diffusion in both the crystal and the electrode, the circuit of fig. 1b has been derived based on electrode reaction (3). It includes separate finite-Warburg impedances for the two diffusion processes. The circuit parameters have the same general form as those given for fig. 1a in eqs. (6)–(10), with, however, the two Warburgs involving two different lengths and two different diffusion coefficients. Preliminary fits for pure β-PbF_2 with Pt electrodes at 314°C yield $R_R = 10\ \Omega$, R_A negligible, $C_A = 68.13\ \mu$F, $Z_{DO,c}/H_c = 963\ \Omega$, H_c very large, $Z_{DO,e}/H_e = 1.70 \times 10^4\ \Omega$, $H_e = 30$ for $P_{O_2} = 40$ Pa, and $R_R = 46.3\ \Omega$, R_A negligible, $C_A = 1.67 \times 10^3\ \mu$F, $Z_{DO,c}/H_c = 1.15 \times 10^3\ \Omega$, H_c very large, $Z_{DO,e}/H_e = 2.53 \times 10^3\ \Omega$, $H_e = 47$ for $P_{O_2} = 1.245$ kPa. The small variation of $Z_{DO,c}/H_c$ with P_{O_2} and the very large value (effectively infinite) for H_c are to be expected for diffusion in the crystal while the decrease in $Z_{DO,e}/H_e$ with P_{O_2}, and the small value of H_e are quite reasonable for diffusion through a very thin electrode. Further details of this model and additional data analysis will be reported at a later date [19].

In comparison with the studies reported by Raistrick et al. [7], and Jonscher and Réau [8], the present study emphasizes the role of oxygen in the interfacial phenomena of some fluorites. The effect could have gone unnoticed in the earlier studies, due to relatively low temperatures, and probably very small oxygen contents in the ambients employed. Moreover, the present study shows that the finite-length War-

burg effects only show up for frequencies lower than $\approx 10^{-2}$ Hz.

Acknowledgement

The authors are indebted to Mr. A. Wolfert, University of Utrecht, for experimental assistance, and to Dr. A. Lehnen, University of North Carolina, for computational assistance. This work has been supported by the US National Science Foundation under Grant Nos. DMR-76-84187, and DMR-80-05236, and by NATO under Research Grant 1696. Additional research support by Memphis State University and its Computing Center is gratefully acknowledged.

References

[1] J.H. Kennedy and R.C. Miles, J. Electrochem. Soc. 123 (1976) 47.
[2] J.M. Réau and J. Portier, in: Solid electrolytes, eds. P. Hagenmuller and W. van Gool (Academic Press, New York, 1978) p. 313.
[3] R.W. Bonne and J. Schoonman, J. Electrochem. Soc. 124 (1977) 28.
[4] G.A. Samara, J. Phys. Chem. Solids 40 (1979) 509.
[5] W.C. Fang and R.A. Rapp, J. Electrochem. Soc. 125 (1978) 683.
[6] R.W. Bonne and J. Schoonman, J. Electrochem. Soc. 125 (1978) 1628.
[7] I.D. Raistrick, C. Ho, Y.W. Hu and R.A. Huggins, J. Electroanal. Chem. 77 (1977) 319.
[8] A.K. Jonscher and J.M. Réau, J. Mat. Sci. 13 (1978) 563.
[9] J.R. Macdonald and M.K. Brachman, Rev. Mod. Phys. 28 (1956) 393.
[10] B.A. Huberman, Phys. Rev. Letters 32 (1974) 1000.
[11] D.R. Franceschetti and J.R. Macdonald, J. Electroanal. Chem. 101 (1979) 307.
[12] J.R. Macdonald, J. Electroanal. Chem. 70 (1976) 17.
[13] J.R. Macdonald and P.W.M. Jacobs, J. Phys. Chem. Solids 37 (1976) 1117.
[14] D.R. Franceschetti and J.R. Macdonald, J. Electroanal. Chem. 82 (1977) 271.
[15] J.R. Macdonald, J. Schoonman and A. Lehnen, to be published.
[16] J.R. Macdonald, J. Electroanal. Chem. 32 (1971) 317.
[17] J.R. Macdonald and J.A. Garber, J. Electrochem. Soc. 124 (1977) 1022.
[18] R. Fletcher and M.J.D. Powell, Computer J. 6 (1963) 163.
[19] D.R. Franceschetti, to be published.